doi:10.1016/j.jmb.2004.05.011 J. Mol. Biol. (2004) 340, 627–637

JMB

Available online at www.sciencedirect.com

SCIENCE DIRECT®

ELSEVIER

Concerted Structural Changes in the Peptidase and the Propeller Domains of Prolyl Oligopeptidase are Required for Substrate Binding

Zoltán Szeltner[1], Dean Rea[2], Tünde Juhász[1], Veronika Renner[1] Vilmos Fülöp[2] and László Polgár[1]*

[1]*Institute of Enzymology Biological Research Center Hungarian Academy of Sciences, H-1518 Budapest 112, P.O. Box 7, Hungary*

[2]*Department of Biological Sciences, University of Warwick, Gibbet Hill Road Coventry CV4 7AL, UK*

**Corresponding author*

Prolyl oligopeptidase contains a peptidase domain and its catalytic triad is covered by the central tunnel of a seven-bladed β-propeller. This domain makes the enzyme an oligopeptidase by excluding large structured peptides from the active site. The apparently rigid crystal structure does not explain how the substrate can approach the catalytic groups. Two possibilities of substrate access were investigated: either blades 1 and 7 of the propeller domain move apart, or the peptidase and/or propeller domains move to create an entry site at the domain interface. Engineering disulfide bridges to the expected oscillating structures prevented such movements, which destroyed the catalytic activity and precluded substrate binding. This indicated that concerted movements of the propeller and the peptidase domains are essential for the enzyme action.

Keywords: substrate binding; site-specific mutagenesis; disulfide bond formation; protein stability

Introduction

A distinct group of serine peptidases cannot hydrolyze proteins, but can readily cleave peptides that are up to about 30 amino acid residues long. These enzymes are grouped under the prolyl oligopeptidase family (S9 of clan SC).[1] Members of the family include dipeptidyl peptidase IV, oligopeptidase B, acylaminoacyl peptidase and the prototype prolyl oligopeptidase, all of which are of physiological and pharmacological importance.[2] Specifically, prolyl oligopeptidase is implicated in a variety of disorders of the central nervous system.[3–6] Inhibitors of the enzyme are described as cognitive enhancers, and some entered clinical trials.[7–10] Dipeptidyl peptidase IV is involved in type 2 diabetes[11–13] and oligopeptidase B in trypanosomiasis.[14–17]

The catalytically competent residues, the so-called catalytic triad (Ser, Asp and His), are concentrated in the carboxyl terminal region, where the amino acid sequence homology is more significant than in the amino-terminal part. The enzymes of the family are much larger (about 80 kDa) than are the classic serine proteases, trypsin and subtilisin (25–30 kDa). The most important structural information was obtained from the 1.4 Å-resolution crystal structure of prolyl oligopeptidase, determined with the native enzyme and its complex with the inhibitor Z-Pro-prolinal (PDB codes 1qfm and 1qfs).[18] The enzyme has a cylindrical shape of an approximate height of 60 Å and diameter of 50 Å. It consists of two domains, a peptidase and a seven-bladed β-propeller.

The peptidase domain is built up of residues 1–72 and 428–710, and the residues between these two portions constitute the propeller domain. In agreement with earlier predictions,[19,20] the peptidase domain exhibits an α/β hydrolase fold characteristic of lipases and other hydrolytic enzymes and contains a central eight-stranded β-sheet with all strands except the second one aligned in a parallel manner. The β-sheet is twisted significantly, and is flanked by two helices on one side and six helices on the other.

The β-propeller of prolyl oligopeptidase is held to the catalytic domain *via* the two connecting

Abbreviations used: Nap, 2-naphthylamide; DTE, 1,4-dithioerythritol; GSSG, oxidized glutathione; Mes, 2-(*N*-morpholino)ethanesulfonic acid; Abz, 2.aminobenzoyl; Phe(NO_2), *p*-nitrophenylalanine.

E-mail address of the corresponding author: polgar@enzim.hu

polypeptide main-chains, with hydrogen bonds and salt bridges, but mainly with hydrophobic forces. The propeller domain is based on a seven-fold repeat of four-stranded antiparallel β-sheets, which are twisted and arranged radially around their central tunnel. They pack face-to-face and the predominantly hydrophobic interaction provides most of the required structural stability. Until recently, all the other known propeller proteins have evolved ways to close the circle ("Velcro") between their first and last blades.[21] In the β-subunit of G proteins, for example, the main-chain hydrogen bonds formed between one β-strand from the amino terminus and three antiparallel β-strands from the carboxyl terminus close the "Velcro". While the six, seven and eight-bladed propellers close the "Velcro" in a similar way,[21,22] the smaller four-bladed proteins (hemopexin and collagenase) form a disulfide bond between the first and last blades.[23–25] The circular structure is not stabilized in prolyl oligopeptidase by these ways. There are only hydrophobic interactions between the first and last blades. Non-velcroed or "open topology" propellers are rare, and prolyl oligopeptidase was the first protein structure exhibiting a domain of this nature. An eight-bladed propeller with open velcro topology was identified during the recent crystal structure determination of the related dipeptidyl peptidase IV enzyme.[26–30] The structures of *Cellvibrio japonicus* α-L-arabininase[31] and *Bacillus subtilis* levansucrase[32] are based on non-velcroed five-bladed propellers. The 720 kDa tricorn protease from *Thermoplasma acidophilum* contains both six and seven-bladed propellers with open velcro topology.[33]

The catalytic triad of prolyl oligopeptidase (Ser554, Asp641, His680) is located in a large cavity at the interface of the two domains.[18] Ser554 is found at the tip of a very sharp turn, referred to as the nucleophile elbow. Consequently, the serine OH group is well exposed and readily accessible to the catalytic imidazole group on one side and to the substrate on the other. His680 is found in the middle of a loop. One of the oxygen atoms of Asp641 is in the plane of the imidazole ring of His680, providing ideal position for hydrogen bond formation.

The narrow entrance of the propeller (~4 Å) opposite to the active site is much smaller than the diameter of an average peptide (6–12 Å), but it could be enlarged by partial separation of the unclosed blades 1 and 7. This process could provide access to the active site for oligopeptides whilst protecting proteins and large structured peptides from accidental hydrolysis. This mechanism was supported by engineering a disulfide bond between blades 1 and 7, which inactivated the enzyme.[34] Specifically, a cysteine residue was substituted for Gln397, because blade 1 already contained a cysteine (Cys78) in an appropriate position to form a disulfide bond with residue 397. Under reducing conditions, the enzyme variant is active but under oxidizing conditions, the activity is lost. The disulfide bond formation was demonstrated by X-ray crystallography.[34] Hence, the regulatory mechanism of prolyl oligopeptidase involves oscillating propeller blades acting as a gating filter during catalysis. It is possible, however, that the opening of the propeller is not full length between the two blades, such that separation of the blades may only be required at either the top of the propeller near the peptidase domain, or the bottom of the propeller at the distal end of the molecule. To test this hypothesis, we have engineered disulfide bonds at each end of the propeller between blades 1 and 7, and analyzed their effects on substrate binding and catalysis.

The prolyl oligopeptidase of the hyperthermophilic *Pyrococcus furiosus* differs from other prolyl oligopeptidases in that it breaks down autocatalytically and hydrolyzes proteins, like azocasein.[35,36] The enzyme is significantly smaller than its mesophilic counterparts. It was suggested that the two domains of the hyperthermophilic enzyme move away from one another and this enables larger protein substrates to approach the active site.[36] Such domain movements may be possible for the mammalian enzyme as well. To test this, a variant was prepared with a movement-restricting disulfide bridge between the domains. Thr597 from the peptidase domain was replaced with cysteine because this residue is well positioned to form a

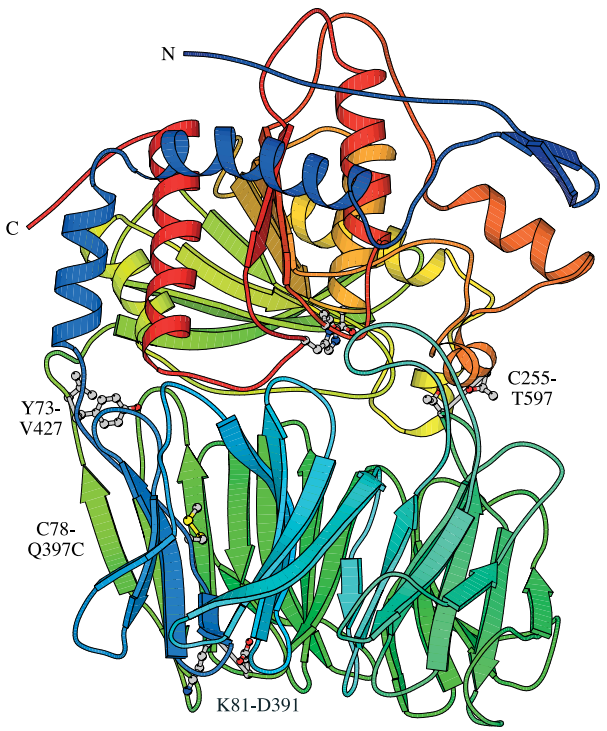

Figure 1. Disulfide bond formation in prolyl oligopeptidase. The potential disulfide engineering sites are shown together with the catalytic triad in the middle of the molecule (drawn from the C255T/C78/Q397C variant, PDB code 1e5t,[34]). The ribbon diagram is colour-ramped blue to red from the N to the C terminus.

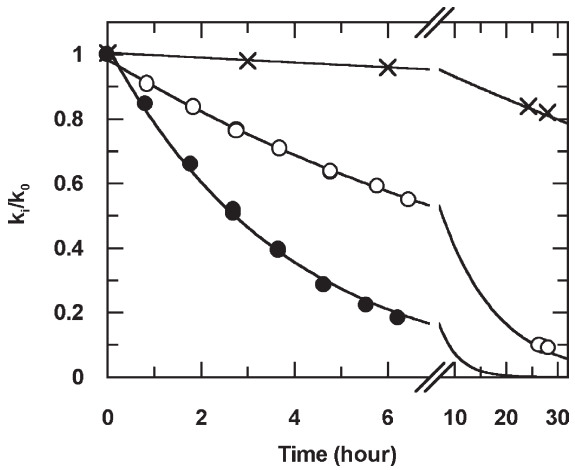

Figure 2. Oxidation of the Y73C/V427C/C255T variant. The reactions were performed at pH 8.5 and 28 °C with air oxygen (×), 0.1 mM GSSG (○), and 0.5 mM GSSG (●). The activities were measured under first-order conditions. k_0 is the first-order rate constant at zero time, k_i refers to the remaining activity at time τ.

disulfide bridge with Cys255 from the propeller domain.

Results

Disulfide bond formations in the propeller domain

To cross-link the potential substrate entrance of prolyl oligopeptidase, we had to introduce cysteine residues into the enzyme. Instead of the wild-type enzyme, we used the C255T enzyme variant because the oxidation of Cys255 or its blocking with glutathione inhibits prolyl oligopeptidase. Cys255 is close to the active site so that a bulky group on its thiol sterically hinders the substrate during the reaction with the catalytic serine.[37] We have prepared the triple mutants Y73C/V427C/C255T and K81C/D391C/C255T and examined to what extent the new cysteine residues influenced the catalytic activity. It was found that the new cysteine residues affected the rate constants only moderately. The location of the disulfide bonds formed after oxidation are illustrated in Figure 1. The oxidations were performed by air or by 0.1 mM and 0.5 mM GSSG, which inactivated the enzyme variants according to first-order reactions. It is seen in Figure 2 and Table 1 that 0.1 mM GSSG, relative to O_2, markedly increases the inactivation rate for the different variants, but the increase in rate constant is not proportional to the concentration of the disulfide compound. Apparently, the rate-limiting step involves a steric component, which makes the large GSSG molecule unable to freely approach the buried cysteine residues. The inactivation rate constants for the control C255T and C255A variants are significantly lower than the corresponding rate constant for Y73C/V427C/C255T. In contrast, the K81C/D391C/C255T variant is more slowly inactivated than the controls (Table 1). In this case, the disulfide bond formation seems to play a minor role in the inactivation. Apparently, the distance between the two residues is not favorable for reaction (see Discussion). Therefore, this enzyme variant was not investigated further.

The slow inactivation of the control enzymes (C255T and C255A) may arise from the reactions with some buried cysteine residues. Blocking the readily available surface cysteine residues with bulky reagents, like *N*-ethyl maleimide, does not affect the activity of the C255T variant.[37] However, during the long incubation employed here, GSSG could react with the hidden cysteine residues, resulting in some distortion in the protein structure. Therefore, we tried cystamine (2,2′-diaminodiethyl disulfide), which being a much smaller compound than GSSG could easier approach the buried cysteine residues. Interestingly, cystamine gave a two-phase inactivation curve with the C255T variant. The activity decreased by about 30% within one minute, and this was followed by a readily measurable single-exponential reaction, the rate constant of which was greater by two orders of magnitude than that of the reaction of GSSG (Table 1). This indicates that: (i) the hidden cysteine residues are not equally accessible for the cystamine, (ii) the reactions of two or more cysteine residues account for the inactivation, reacting slower and faster with cystamine, and (iii) the inactivation is much faster with the smaller cystamine than with GSSG.

X-ray crystallography demonstrated the formation of the disulfide bond in the Y73C/V427C/C255T variant (Figure 3(A)). This is the linker

Table 1. Rate constants of inactivation (pH 8.5)

Variant	O_2 10^3k (h^{-1})	0.1 mM GSSG 10^3k (h^{-1})	0.5 mM GSSG 10^3k (h^{-1})	0.1 mM CA,[a] 10^3k (h^{-1})
C255A		54.4 ± 1.0	128.9 ± 7.1	
C255T		56.5 ± 0.9	112.9 ± 2.2	7990 ± 600
Y73C/V427C/C255T	15.3 ± 0.8	91.8 ± 1.7	264.1 ± 6.3	
K81C/D391C/C255T		36.9 ± 1.1	72.2 ± 1.6	
C78A/C255T		47.0 ± 0.8	108.0 ± 1.7	7400 ± 400
T597C	20.3 ± 0.7	355 ± 7	1344 ± 27	>30,000

[a] CA = cystamine. Rate constants refer to the slow phase.

region between the two domains and normally shows high flexibility and consequently poor electron density between residues 70–76 and 424–430. Upon disulfide formation, a slightly different conformation is adopted with respect to the wild-type enzyme (PDB code 1h2w). The C^{α} atoms have an rms deviation of 1.41 Å (0.37 Å for all 710 residues). Subsequently, the main-chain gets more ordered and the temperature factor ratio between the C^{α} atoms of this region and the whole molecule is 1.38, which is significantly lower than the corresponding figure of 1.83 for the wild-type structure.

The K81C/D391C/C255T variant did not prove to be a good disulfide forming species. Catalytic activity was lost under oxidative conditions even slower than the controls C255A and C255T (Table 1). This unexpected result may be due to some changes in the structure of the modified protein because Asp391 OD2 forms a hydrogen bond with the main-chain NH of Gln388, and this structurally influential bond disappears when cysteine replaces Asp391. In addition, Lys81 and Asp391 seem to be important for the folding of the protein because most of the K81C/D391C/C255T variant is produced as inclusion bodies, and only a small fraction is obtained in the soluble form. Furthermore, the distance between the cysteine residues is not optimal (see Discussion).

Cross-linking the propeller and peptidase domains

The role of possible domain fluctuations during substrate entry was explored by introducing a disulfide bond between the peptidase and the propeller to prevent the required domain motions. To this end Thr597 of the peptidase domain was mutated to cysteine, since this residue assumed a favorable position to form a disulfide bond with Cys255 of the propeller domain.

The reduced form was slowly oxidized by air at 28 °C and at pH 8.5. The decrease in activity followed a single exponential decay (Figure 4). No appreciable decrease in the activity of the C255A variant was observed (Figure 4). This control was used instead of the wild-type enzyme, as the

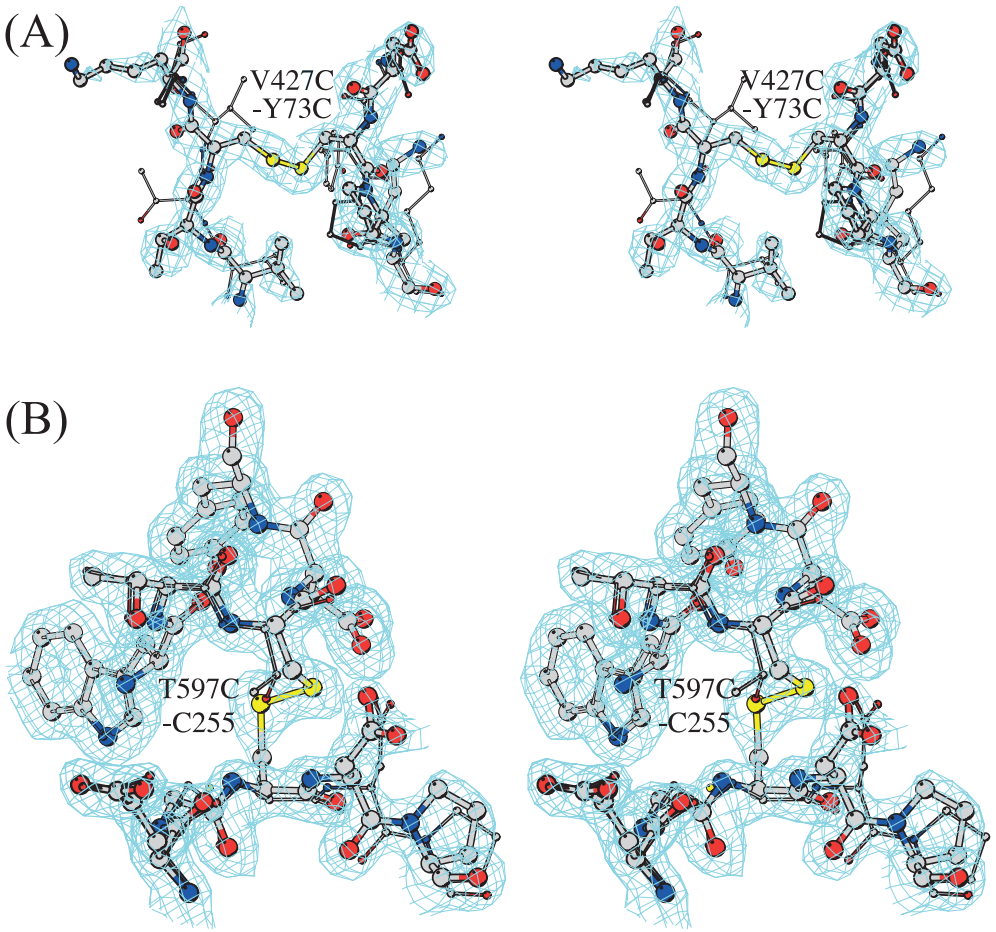

Figure 3. Stereo view of the disulfide bond formation in prolyl oligopeptidase. Electron density around the disulfide bonds Y73C-V427C (A) and C255-T597C (B). The SIGMAA[51] weighted $2mF_o - \Delta F_c$ electron density using phases from the final model is contoured at 1σ level, where σ represents the rms electron density for the unit cell. Contours more than 1.4 Å from any of the displayed atoms have been removed for clarity. Residues of the wild-type enzyme are shown as thin lines (from PDB entry 1h2w) (drawn with MolScript[52,53]).

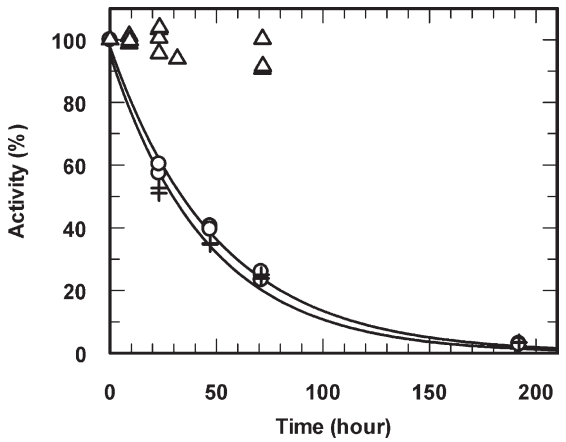

Figure 4. Oxidation of prolyl oligopeptidase variants by air. The activity of the T597C variant was measured with Z-Gly-Pro-Nap (○) or Abz-Gly-Phe-Gly-Pro-Phe-Gly-Phe(NO_2)-Ala-NH_2 (+). The C255A variant was used as control (△).

oxidation of Cys255, which is close to the binding site, may also reduce the catalytic activity.[37] The results have suggested that the prevention of domain motions almost completely inhibited the activity. The activity of the oxidized enzyme was regained by incubation with 1.5 mM DTE at pH 8.5 (Figure 5), supporting that the loss of activity was associated with the disulfide formation. The formation of the disulfide bond was verified by X-ray crystallography (Figure 3(B)), which showed that the structure was not significantly perturbed with respect to the wild-type enzyme (PDB code 1h2w). The rms deviation was 0.17 Å for all the 710 fitted C^{α} atoms, and this was only slightly higher, 0.46 Å, for the shown region between residues 253–257 and 595–599.

The very slow reaction with oxygen did not permit to complete fully the oxidation. The remaining activity was shown to originate from the reduced form. Specifically, maleimide inhibits prolyl oligopeptidase by about 85%, when it reacts with Cys255.[37] After four days of incubation, the remaining activity could be inhibited with maleimide to a similar extent, which clearly indicated that the activity originated from the reduced enzyme present in the incompletely oxidized sample. Addition of 0.05–0.1 mM GSSG accelerated the formation of the disulfide bond. However, the oxidizing agent, as shown above, can also react with the thiol groups on the surface of prolyl oligopeptidase. To reduce the possibility of such undesirable reactions, we did not use a large excess of oxidizing agent.

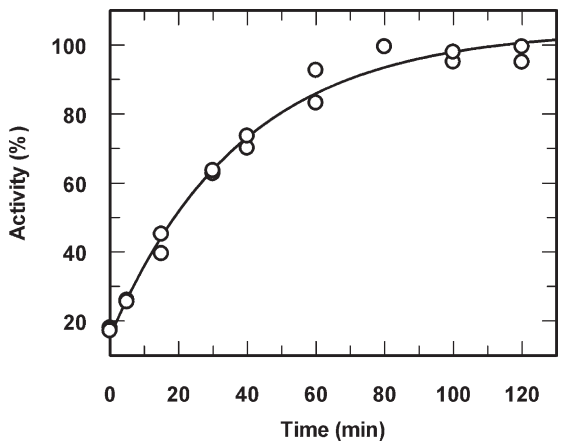

Figure 5. Reactivation of the oxidized T597C variant of prolyl oligopeptidase. Reduction of the disulfide bond was achieved with 1.5 mM DTE.

Disulfide bond increases protein stability

We have investigated whether or not the formation of the disulfide bond modifies the stability of the enzyme. Figure 6 illustrates the temperature scans of the T597C and the C255A variants, the latter being unable to form a disulfide bridge. Both the reduced and oxidized forms of the control C255A enzyme gave similar curves displaying two peaks, a smaller (t_m1) and a larger (t_m2) at lower and higher temperature, respectively (Table 2). A similar curve was obtained with the wild-type enzyme (not shown). However, the air-oxidized T597C with 22% remaining activity exhibited three peaks. The additional peak was formed at the highest temperature (t_m3). The 7.0 °C shift from t_m2 indicates that the disulfide bond has generated significant stabilization in the protein structure. Another sample incubated overnight in the presence of 50 μM GSSG (broken line in Figure 6) retained 10% activity. As seen, the change in protein stability was practically independent of whether the oxidation was achieved by GSSG or oxygen. The new peak apparently formed in concert with the generation of the disulfide bond. At the start of the oxidation a shoulder to the second peak (t_m2) developed (not shown), which gradually enlarged as the oxidation proceeded. Similar stabilization was obtained with the Y73C/V427C/C255T variant (Table 2). However, with this variant the first peak practically disappeared during oxidation. A similar phenomenon was observed when blades 1 and 7 were cross-linked with the disulfide bond between residues 78 and 397.[34] A further difference associated with the Y73C/V427C/C255T variant is the lower t_m values. This is due to the insertion of either Cys73 or Cys427, both resulting in labilization of the protein structure as indicated by the lower t_m values of the double mutants Y73C/C255T and V427C/C255T (Table 2). The labilization is greater when both cysteine residues are present (Y73C/V427C/C255T).

Disulfide bond impedes substrate binding

Whether the lack of activity arises from the inability of the substrate to enter the cavity of the cross-linked enzyme was examined by substrate

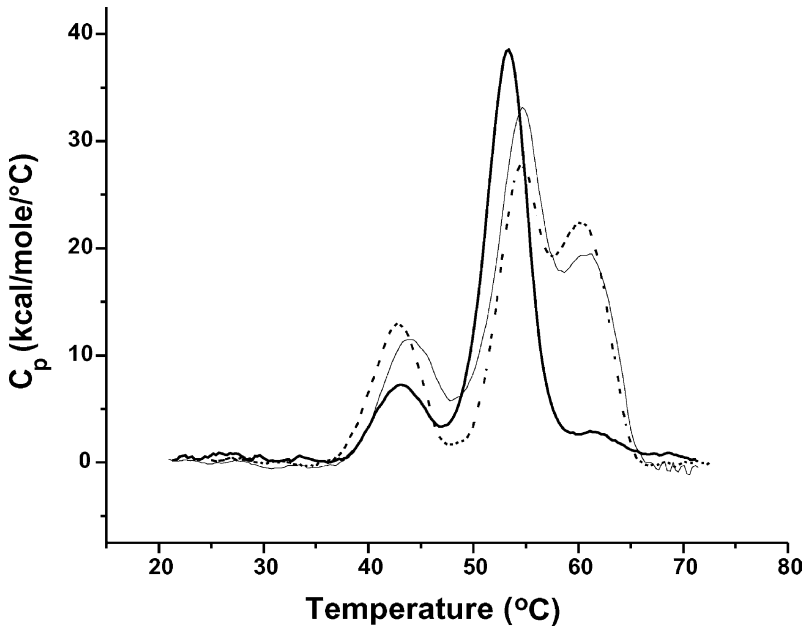

Figure 6. DSC scans of oxidized prolyl oligopeptidase variants. Thick curve, air-oxidized C255A variant; thin line, air-oxidized T597C variant; broken line, T597C variant oxidized with 50 μM GSSG.

binding studies. To this end, a modified oxidized enzyme was used (S554A/T597C), in which the catalytic serine was abolished to prevent substrate hydrolysis. It has already been shown that the internally fluorescent substrate, Abz-Gly-Phe-Gly-Pro-Phe-Gly-Phe(NO_2)-Ala-NH_2 readily binds to the inactive S554A variant.[38] However, there was no substrate binding with the oxidized S554A/T597C enzyme, except with about 20% of reduced enzyme, which was still present after an overnight incubation with 0.05 mM GSSG. The difference in binding between the reduced and oxidized enzymes was demonstrated by adding an excess of enzyme to the substrate and measuring the resulting fluorescence intensity. The S554A variant, not containing the disulfide bond, was used as a control. The enzyme concentration employed (140 μM) was not enough to convert the substrate completely into enzyme–substrate complex. The saturation was about 80% under the experimental conditions, as indicated by the extrapolated fluorescence value of the titration curve (390 fluorescence units) determined as described.[38] Nonetheless, the fluorescence of the complex of the oxidized S554A/T597C enzyme is much less (61 units) than that of the reduced (285 units) and the C554A variants (300). At full saturation, the fluorescence is similar to that obtained during substrate hydrolysis,[38] where the donor and acceptor groups are separated. In the enzyme–substrate complex only the P3-P2′ residues are bound. The fluorophore (P5) and the quenching (P3′) groups are disordered, not seen in the electron density map. A direct intramolecular encounter of the two remote groups is not possible. The small difference between the reduced S554A/T597C and the C255A variants (300 − 285 = 15) may be due to a somewhat higher dissociation constant formed with the former (52 ± 4 μM) than with the latter enzyme–substrate complex (40 ± 1 μM). These results indicate that the substrate cannot enter the cavity of the cross-linked protein, and this explains why the oxidized enzyme does not show an appreciable activity.

Table 2. t_m values for prolyl oligopeptidase variants

	Reduced			Oxidized		
Enzyme	t_m1	t_m2	t_m3	t_m1	t_m2	t_m3
T597C	43.7	53.5	–	43.6[a]	53.6[a]	60.5[a]
T597C	43.6	53.5	–	43.6[b]	53.6[b]	60.4[b]
C255A	43.7	53.5	–	43.4[a]	52.4[a]	–
C255T	44.3	52.0	–			
Wild-type	44.0	53.6	–			
Y73C/V427C/C255T	40.3	50.2	–	–	51.6[b]	58.2[b]
Y73C/C255T	41.8	51.9	–			
V427C/C255T	41.8	51.9	–			

[a] Oxidized by air.
[b] Oxidized by 50 μM GSSG.

Discussion

The crystal structure of prolyl oligopeptidase displays an apparently firm two-domain construction, which should exclude even the smallest peptide from the active site. Catalysis of the highly efficient prolyl oligopeptidase requires very rapid conformational changes that open up the enzyme structure between blades 1 and 7, between the propeller and the peptidase domains, or presumably at both parts of the structure. To distinguish between the potential mechanisms, we have suppressed the oscillation dynamics by introducing disulfide bridges at the possible substrate entry sites. The rates for the various bond formations were rather different: four- to fivefold higher for the C255–T597C (propeller-peptidase) than for the formation of the Y73C-V427C bond (blade

1–blade 7, close to the peptidase domain). Interestingly, the formation of the K81C–D391C bond (blade 1–blade 7, distant from the peptidase domain) was even slower (Table 1) than the inactivation of the control enzyme variant that is unable to form a disulfide bond. The inactivation was likely due to the reaction of some buried cysteine residues of the protein since their blocking can distort the protein structure. The size of the oxidizing agent is of primary importance, which is obvious from the rapid reaction with the small cystamine (Table 1). A different type of reaction with the small oxygen molecule, however, was slower than that of the GSSG reaction. The concentration of oxygen did not limit the reaction under the conditions employed because the inactivation rate constant remained unchanged at a tenfold enzyme concentration.

Two additional factors can be considered in disulfide bond formation. (i) The distance between the C^{α} atoms of the two cysteine residues involved in cross-linking. Theoretically, the distance can range from about 4 Å to 9 Å. However, the effective range is narrower, since most of the disulfides observed in proteins fall between 4.4 Å and 6.8 Å.[39] As seen in Table 3, the K81C/D391C/C255T variant (7.74 Å) overextends the effective range, whereas the Y73C/V427C/C255T enzyme (6.41 Å) is a fairly good candidate for forming a disulfide bond, as observed here. The C255/T597C variant is even more favorable (5.85 Å), and this is consistent with the high rate constant for the reaction with GSSG (last row of Table 1). (ii) A further way of estimating the possibility of disulfide bond formation considers the amino acid sequences around the cysteine residues (ten residues on each side of the cysteine). It has previously been shown that the sequential environments of free cysteine residues and half cystines are different, which distinguishes the two species in natural proteins.[40] For example, Gly is the most abundant in the vicinity of half cystines. Using that method, we calculated the preferences for disulfide formation. The values are shown in Table 3, where the unit value represents 50–50% of the two oxidation states. It is seen that the disulfide would most probably be formed in the Y73C/V427C/C255T variant and less probably in the K81C/D391C/C255T variant. Other potential disulfides are also shown in Table 3. In agreement with the experimental data, the Y73C/V427C/C255T variant would be more likely to form a disulphide than the K81C/D391C/C255T variant if either the sequence surrounding the cysteine residues or the distance between the C^{α} atoms is considered.

Table 3. Factors affecting potential disulfide bond formations

Disulfide	Distance (Å)[a]	Potential[b]
Y73-V427	6.41	9.28
K81-D391	7.74	2.98
C78-Q397	6.27	2.95
C255-T597	5.85	0.08
L70-V486	6.78	0.96
L94-T686	6.38	0.09
F401-V455	7.69	0.04

[a] Distance between the C^{α} atoms.
[b] Calculated from amino acid sequence as described by Fiser *et al.*[40] Higher potential suggests higher probability of disulfide formation.

The above results indicate that flexibility of propeller blades 1 and 7 is required for enzyme activity. Separation of the peptidase and the propeller domains is similarly required, not just for enzyme activity but for substrate entry into the enzyme cavity. This suggests a mechanism in which substrate entry requires a concerted action of the propeller blades and the domains. This is conceivable since the blades are coupled not only with one another but also with the peptidase domain. There is 2545 $Å^2$ of inaccessible surface area buried between the propeller and the peptidase domain. Because the domains are in such close contact, some motion in the propeller is required for loosening the interaction between the propeller and the peptidase domains. This explains the need for domain flexibility and the loss of activity of the T597C variant in oxidizing conditions, where a disulfide bridge between the domains prevents the required domain movements.

Prolyl oligopeptidase was the first example of a protein containing a β-propeller with open-velcro topology. The recent structure determination of the related dipeptidyl peptidase IV revealed this enzyme also has a propeller of open-velcro topology, albeit eight-bladed[26–30] instead of seven-bladed as observed in prolyl oligopeptidase. However, the mechanism of substrate entry into the cavity of dipeptidyl peptidase IV differs to that of prolyl oligopeptidase. There are two tunnels to the active site of dipeptidyl peptidase IV and both are large enough to allow passage of a substrate without the need for conformational changes. This structure thus fails to shed any light on the probable substrate entry site of prolyl oligopeptidase, but it is another possible example of substrate access to a buried active site through an open-topology β-propeller.

The crystal structure of tricorn protease revealed an enzyme with two open-topology β-propellers.[33] Seven and six-bladed propellers provide a separate entrance to and exit from the active site, respectively.[41,42] Peptides produced by tricorn protease must be further degraded into smaller products by other peptidases. One such enzyme is the tricorn interacting peptidase F1 that cleaves the small peptides produced by tricorn protease into single amino acid residues.[43] The catalytic domain of F1 has α/β hydrolase topology and superimposes very well onto the peptidase domain of prolyl oligopeptidase. F1 also has separate substrate entry and product exit sites, though not *via* open-topology β-propellers. The structure of

F1 suggests a possible functional complex in which the substrate entry tunnel of F1 aligns with the product exit tunnel of tricorn protease, allowing efficient processive degradation to free amino acid residues for cellular recycling of proteins.

The finding of two dynamic openings in prolyl oligopeptidase, i.e. between the first and last blades, and between the peptidase and propeller domains, raises the possibility of separate substrate entry and product exit sites in this enzyme, as suggested for dipeptidyl peptidase IV, tricorn and F1 peptidases. This mechanism could promote prolyl oligopeptidase catalysis, if the substrate enters and the product exits during a singly concerted structural movement. Unfortunately, these structural movements proved to be too great to be accommodated in the crystal lattice: all soaking experiments with ligands/substrates/products/inhibitors destroyed the crystal lattice, hence co-crystallization experiments had to be carried out to obtain enzyme–ligand complexes.

We have recently prepared the propeller domain in isolation from the peptidase domain. The isolated propeller domain proved to be more stable than the intact enzyme, as demonstrated by differential scanning calorimetry (data not shown). This indicates that the interaction between blades 1 and 7 is rather strong even in the absence of a "Velcro". This supports passage between the domains as the primary route for substrate communication. However, the requirement for blade separation, as demonstrated by the Y73C/V427C/C255T and Q397C mutants, suggests a concerted movement involving domain motions and distortion of the propeller during substrate entry and/or product exit.

Materials and Methods

Preparation of prolyl oligopeptidase variants

Prolyl oligopeptidase from porcine brain and its variants were expressed in *Escherichia coli* JM105 cells and purified as described.[44] Its C255A and C255T variants were prepared similarly.[37]

Mutation for the T597C variant was introduced with the two-step polymerase chain reaction (PCR) technique as described for the Y473F mutant.[44] In short, four oligonucleotides were synthesized to produce the T597C mutant. The oligonucleotides designed to the 5′ and 3′-ends of the gene contained EcoRI and KpnI restriction sites (underlined), respectively, while the mutagenic primers with the TGC codon for cysteine had an NsiI site (underlined):

To the 5′-end:	5′-GCAGGAATTCTAAGGAGGAATT-3′
To the 3′-end:	5′-CGGGGTACCTTACGGAATCCAGTC GATGTTCAG-3′
Sense primer:	5′-GGTCATGCAtGGACCtgCGATTATG GG-3′
Antisense primer:	5′-CCCATAATCGcaGGTCC*aTGCAT*GA CC-3′

In the first step of PCR two independent reactions were carried out, using the Vent polymerase and the pTrc/POP plasmid as template, digested with KpnI enzyme. To this mixture were added the 5′-primer and the antisense mutagenic primer in the first reaction. In the second reaction the 3′-primer and the sense mutagenic primer were applied, using 26 cycles in each run. The mutated gene was then obtained in two pieces, which were isolated by agarose gel electrophoresis. This was followed by purification using a QIAquick Gel Extraction Kit. In the second step, the combined two gene fragments were used as templates, and the reaction mixture was heated to 95 °C prior to the addition of the Vent polymerase. The temperature was then lowered to 55 °C, while the complementary ends of the two DNA portions formed double stranded DNA. The complementary strands were synthesized during heating at 72 °C for five minutes. The complete strands were able to bind the terminal primers (5′ and 3′ primers to the 5′ and 3′ termini of the gene, respectively), which were added to the mixture at 95 °C. The amplification was then carried out in 30 cycles at 95 °C, 55 °C, and 72 °C for 1 minute, 1 minute, and 2.5 minutes, respectively. The PCR product was identified on a 1% (w/v) agarose gel and purified with the QIAquick Gel Extraction Kit. The pure product was digested with EcoRI and KpnI restriction enzymes and isolated with agarose gel electrophoresis. Then it was ligated into an empty pTrc99A vector digested with EcoRI and KpnI enzymes. The T597C mutation was verified by digestion with NsiI enzyme. The T597C variant was expressed and purified like the wild-type prolyl oligopeptidase.

The double mutant T597C/S554A was constructed by subcloning the EcoRI-StuI fragment (that contained the mutation) from the T597C construct to the place of the EcoRI-StuI fragment of the S554A variant of prolyl oligopeptidase. The expression and purification were carried out as with the T597C variant, except that the purification of the inactive enzyme was followed by SDS gel electrophoresis.

The Y73C, V427C, K81C and D391C mutations were introduced individually into the prolyl oligopeptidase gene with the C255A mutation in the pTrc99A plasmid, which was used as template in the two-step PCR procedure described above.

The Y73C and K81C mutations reside between the EcoRI and BsmI sites of the gene. These EcoRI-BsmI fragments, containing the Y73C or the K81C mutation, were subcloned to the place of the EcoRI-BsmI fragments of the clones that contained the V427C/C255T or the D391C/C255T mutation, which resulted in the Y73C/V427C/C255T and K81C/D391C/C255T triple mutants. Restriction digestions and sequence analyses using the mutagenic and the 5′ and the 3′-primers verified the mutations.

Disulfide bond formation

Oxidation by air of the thiol groups to form a disulfide bridge was performed in a closed 500 ml centrifuge tube. The reaction mixture (8.0 ml) contained 5.0 μM enzyme and was incubated at 28 °C in 50 mM Tris (pH 8.5), containing 1 mM EDTA. Aliquots were withdrawn from the reaction mixture at appropriate times and the change in the enzyme activity was measured with Z-Gly-Pro-Nap substrate. In the case of the inactive enzyme, which was also modified at the catalytic serine (S554A/T597C), we used the active enzyme (T597C) as a control to estimate

the progress of oxidation during the course of incubation. Oxidation with GSSG was achieved in 1 ml of reaction mixture using small vials.

Kinetic measurements

The reaction of prolyl oligopeptidase with Z-Gly-Pro-Nap (Bachem Ltd., Bubendorf, Switzerland) was measured fluorometrically, using a Cary Eclipse fluorescence spectrophotometer equipped with a Peltier four-position multicell holder accessory and a temperature controller. The excitation and emission wavelengths were 340 nm and 410 nm, respectively. Cells with excitation and emission path-lengths of 1.0 cm and 0.4 cm, respectively, were used. The substrate with internally quenched fluorescence, Abz-Gly-Phe-Gly-Pro-Phe-Gly-Phe(NO_2)-Ala-NH_2, was prepared with solid phase synthesis, and its hydrolysis was followed as in the case of Z-Gly-Pro-Nap, except that the excitation and emission wavelengths were 337 nm and 420 nm, respectively.

For comparison of the activities of the different enzyme variants the specificity rate constants, k_{cat}/K_m, were used at the pH optimum. To this end, the pH dependence of the rate constants was measured at 25 °C in a buffer containing 25 mM acetic acid, 25 mM Mes, 25 mM glycine, 75 mM Tris, and 1 mM EDTA (standard buffer), adjusted to the required pH by the addition of 1 M NaOH or 1 M HCl. Theoretical curves for bell-shaped pH-rate profiles were calculated by non-linear regression analysis, using the GraFit software.[45]

Substrate binding to the cross-linked enzyme

The oxidized T597C/S554A enzyme variant was prepared in the presence of 50 μM of GSSG using an overnight incubation at 28 °C. To the internally quenched substrate, Abz-Gly-Phe-Gly-Pro-Phe-Gly-Phe(NO_2)-Ala-NH_2, in the standard buffer (pH 8.0), was given an excess of the oxidized enzyme, and the increase in fluorescence was recorded.[38]

Crystallization, X-ray data collection and structure refinement

The Y73C/V427C/C255T and T597C/C255 variants of prolyl oligopeptidase were crystallized using the conditions established for the wild-type enzyme except 1 mM oxidized glutathione was included in the mother liquor.[18] Crystals belong to the orthorhombic space group $P2_12_12_1$. X-ray diffraction data were collected using synchrotron radiation. Data were processed using the HKL suite of programs.[46] Refinement of the structures was carried out by alternate cycles of REFMAC[47] and manual refitting using O,[48] based on the 1.4 Å resolution model of wild-type enzyme[49] (PDB code: 1h2w). Water molecules were added to the atomic model automatically using ARP[50] at the positions of large positive peaks in the difference electron density, only at places where the resulting water molecule fell into an appropriate hydrogen-bonding environment. Restrained isotropic temperature factor refinements were carried out for each individual atom. Data collection and refinement statistics are given in Table 4.

Protein Data Bank accession numbers

The coordinates and structure factors have been deposited in the RCSB Protein Data Bank as 1VZ2 and 1VZ3.

Table 4. Data collection and refinement statistics

	Y73C/V427C/C255T	T597C/C255
Data collection		
Synchrotron radiation, detector and wavelength (Å)	SRS 14.1 ADSC Q4 CCD 1.488	SRS 14.1 ADSC Q4 CCD 1.488
Unit cell (Å)	70.9, 99.6, 110.0	71.4, 100.5, 111.8
Resolution (Å)	36–2.2 (2.28–2.20)	26–1.6 (1.66–1.60)
Observations	151,449	394,876
Unique reflections	39,994	105,437
$I/\sigma(I)$	16.4 (4.4)	23.3 (3.2)
R_{sym}[a]	0.081 (0.185)	0.060 (0.216)
Completeness (%)	99.4 (95.1)	99.0 (99.3)
Refinement		
Non-hydrogen atoms	6231 (including 5 glycerol and 506 water molecules)	6891 (including 5 glycerol and 1161 water molecules)
R_{cryst}[b]	0.163 (0.176)	0.160 (0.234)
Reflections used	38,300 (2,675)	101,129 (7,346)
R_{free}[c]	0.208 (0.209)	0.193 (0.288)
Reflections used	1694 (102)	4308 (325)
R_{cryst} (all data)[b]	0.165	0.161
Mean temperature factor (Å^2)	25.2	21.5
rmsds from ideal values		
Bonds (Å)	0.010	0.013
Angles (deg.)	1.2	1.4
DPI coordinate error (Å)	0.25	0.08

Numbers in parentheses refer to values in the highest resolution shell.
[a] $R_{sym} = \sum_j \sum_h |I_{h,j} - \langle I_h \rangle| / \sum_j \sum_h \langle I_h \rangle$ where $I_{h,j}$ is the jth observation of reflection h, and $\langle I_h \rangle$ is the mean intensity of that reflection.
[b] $R_{cryst} = \sum ||F_{obs}| - |F_{calc}|| / \sum |F_{obs}|$ where F_{obs} and F_{calc} are the observed and calculated structure factor amplitudes, respectively.
[c] R_{free} is equivalent to R_{cryst} for a 4% subset of reflections not used in the refinement.[54]

Acknowledgements

This work was supported by the Wellcome Trust (grant no. 060923/Z/00/Z and 066099/01/Z) and the Human Frontier Science Program (RG0043/2000-M 102). V.F. is a Royal Society University Research Fellow. Thanks are due to Ms I. Szamosi for excellent technical assistance. D.R. thanks the BBSRC for the award of a studentship. We are grateful for access to the synchrotron facilities of SRS, Daresbury (U.K.).

References

1. Rawlings, N. D. & Barrett, A. J. (1994). Families of serine peptidases. *Methods Enzymol.* **244**, 19–61.
2. Polgár, L. (2002). The prolyl oligopeptidase family. *Cell. Mol. Life Sci.* **57**, 349–362.
3. Polgár, L. (2002). Structure–function of prolyl oligopeptidase and its role in neurological disorders. *Curr. Med. Chem.-Central Nervous System Agents*, **2**, 251–257.
4. Williams, R. J., Cheng, L., Mudge, A. W. & Harwood, A. J. (2002). A common mechanism of action for three mood-stabilizing drugs. *Nature*, **417**, 292–295.
5. Schulz, I., Gerhartz, B., Neubauer, A., Holloschi, A., Heiser, U., Hafner, M. & Demuth, H.-U. (2000). Modulation of inositol 1,4,5-triphosphate concentration by prolyl endopeptidase inhibition. *Eur. J. Biochem.* **269**, 5813–5820.
6. Harwood, A. J. (2003). Neurodevelopment and mood stabilizers. *Curr. Mol. Med.* **3**, 472–482.
7. Cacabelos, R., Alvarez, A., Lombardi, V., Fernández-Novoa, L., Corzo, L., Pérez, P. *et al.* (2000). Pharmacological treatment of Alzheimer disease: from psychotropic drugs and cholinesterase inhibitors to pharmacogenomics. *Drugs Today*, **36**, 415–499.
8. Morain, P., Robin, J. L., De Nanteuil, G., Jochemsen, R., Heidet, V. & Guez, D. (2000). Pharmacodynamic and pharmacokinetic profile of S 17092, a new orally active prolyl endopeptidase inhibitor, in elderly healthy volunteers. A phase I study. *Br. J. Clin. Pharmacol.* **50**, 350–359.
9. Morain, P., Lestage, P., De Nanteuil, G., Jochemsen, R., Robin, J. L., Guez, I. & Boyer, P. A. (2002). S 17092: a prolyl endopeptidase inhibitor as a potential therapeutic drug for memory impairment. Preclinical and clinical studies. *CNS Drug Rev.* **8**, 31–52.
10. Bellemere, G., Morain, P., Vaudry, H. & Jeugou, S. (2003). Effect of S 17092, a novel prolyl endopeptidase inhibitor, on substance P and alpha-melanocyte-stimulating hormone breakdown in the rat brain. *J. Neurochem.* **84**, 919–929.
11. Drucker, D. J. (2001). Minireview: the glucagon-like peptides. *Endocrinology*, **142**, 521–527.
12. Vilsboll, T., Krarup, T., Deacon, C. F., Madsbad, S. & Holst, J. (2001). Reduced postprandial concentrations of intact biologically active glucagon-like peptide 1 in type 2 diabetic patients. *Diabetes*, **50**, 609–613.
13. Rosenblum, J. S. & Kozarich, J. W. (2003). Prolyl peptidases: a serine peptidase subfamily with high potential for drug discovery. *Curr. Opin. Chem. Biol.* **7**, 496–504.
14. Caler, E. V., de Avalos, S. V., Haynes, P. A., Andrews, N. W. & Burleigh, B. A. (1998). Oligopeptidase B-dependent signaling mediates host cell invasion by *Trypanosoma cruzi*. *EMBO J.* **17**, 4975–4986.
15. Morty, R. E., Lonsdale-Eccles, J. D., Mentele, R., Auerswald, E. A. & Coetzer, T. H. (2001). Trypanosome-derived oligopeptidase B is released into the plasma of infected rodents, where it persists and retains full catalytic activity. *Infect. Immun.* **68**, 2757–2761.
16. Burleigh, B. A. & Woolsey, A. M. (2002). Cell signalling and *Trypanosoma cruzi* invasion. *Cell Microbiol.* **4**, 701–711.
17. Cazzulo, J. J. (2002). Proteinases of *Trypanosoma cruzi*: potential targets for the chemotherapy of Chagas disease. *Curr. Top. Med. Chem.* **2**, 1261–1271.
18. Fülöp, V., Böcskei, Z. & Polgár, L. (1998). Prolyl oligopeptidase: an unusual β-propeller domain regulates proteolysis. *Cell*, **94**, 161–170.
19. Polgár, L. (1992). Structural relationship between lipases and peptidases of the prolyl oligopeptidase family. *FEBS Letters*, **311**, 281–284.
20. Goossens, F., De Meester, I., Vanhoof, G., Hendricks, D., Vriend, G. & Scharpé, S. (1995). The purification, characterization and analysis of primary and secondary-structure of prolyl oligopeptidase from human lymphocytes. Evidence that the enzyme belongs to the α/β hydrolase fold family. *Eur. J. Biochem.* **233**, 432–441.
21. Fülöp, V. & Jones, D. T. (1999). β propellers: structural rigidity and functional diversity. *Curr. Opin. Struct. Biol.* **9**, 715–721.
22. Baker, S. C., Saunders, N. F. W., Willis, A. C., Ferguson, S. J., Hajdu, J. & Fülöp, V. (1997). Cytochrome cd1 structure: unusual haem environments in a nitrite reductase and analysis of factors contributing to β-propeller folds. *J. Mol. Biol.* **269**, 440–455.
23. Faber, H. R., Groom, C. R., Baker, H. M., Morgan, W. T., Smith, A. & Baker, E. N. (1995). 1.8 Å crystal structure of the C-terminal domain of rabbit serum haemopexin. *Structure*, **3**, 551–559.
24. Li, J., Brick, P., O'Hare, M. C., Skarzynski, T., Lloyd, L. F., Curry, V. *et al.* (1995). Structure of full-length porcine synovial collagenase reveals a C-terminal domain containing a calcium-linked, four-bladed β-propeller. *Structure*, **3**, 541–549.
25. Paoli, M., Anderson, B. F., Baker, H. M., Morgan, W. T., Smith, A. & Baker, E. N. (1999). Crystal structure of hemopexin reveals a novel high-affinity heme site formed between two β-propeller domains. *Nature Struct. Biol.* **6**, 926–931.
26. Engel, M., Hoffmann, T., Wagner, L., Wermann, M., Heiser, U., Kiefersauer, R. *et al.* (2003). The crystal structure of dipeptidyl peptidase IV (CD26) reveals its functional regulation and enzymatic mechanism. *Proc. Natl Acad. Sci.* **100**, 5063–5068.
27. Hiramatsu, H., Kyono, K., Higashiyama, Y., Fukushima, C., Shima, H., Sugiyama, S. *et al.* (2003). The structure and function of human dipeptidyl peptidase IV, possessing a unique eight-bladed β-propeller fold. *Biochim. Biophys. Res. Commun.* **302**, 849–854.
28. Oefner, C., D'Arcy, A., Mac Sweeney, A., Pierau, S., Gardiner, R. & Dale, G. E. (2003). High-resolution structure of human apo dipeptidyl peptidase IV/CD26 and its complex with 1-[([2-[(5-iodopyridin-2-yl)amino]-ethyl]amino)-acetyl]-2-cyano-(S)-pyrrolidine. *Acta Crystallog. sect. D*, **59**, 1206–1212.
29. Rasmussen, H. B., Branner, S., Wiberg, F. C. & Wagtmann, N. (2003). Crystal structure of human dipeptidyl peptidase IV/CD26 in complex with a substrate analog. *Nature Struct. Biol.* **10**, 19–25.
30. Thoma, R., Loffler, B., Stihle, M., Huber, W., Ruf, A.

& Hennig, M. (2003). Structural basis of proline-specific exopeptidase activity as observed in human dipeptidyl peptidase-IV. *Structure*, **8**, 947–959.
31. Nurizzo, D., Turkenburg, J. P., Charnock, S., Roberts, S. M., Dodson, E. J., McKie, V. A. *et al.* (2002). *Cellvibrio japonicus* (-L-arabinanase 43A has a novel five-blade β-propeller fold. *Nature Struct. Biol.* **9**, 665–668.
32. Meng, G. & Futterer, K. (2003). Structural framework of fructosyl transfer in *Bacillus subtilis* levansucrase. *Nature Struct. Biol.* **10**, 935–941.
33. Brandstetter, H., Kim, J. S., Groll, M. & Huber, R. (2001). Crystal structure of the tricorn protease reveals a protein disassembly line. *Nature*, **414**, 466–470.
34. Fülöp, V., Szeltner, Z. & Polgár, L. (2000). Catalysis of serine oligopeptidases is controlled by a gating filter mechanism. *EMBO Rep.* **1**, 277–281.
35. Harwood, V. J. & Schreier, H. J. (2001). Prolyl oligopeptidase from *Pyrococcus furiosus*. *Methods Enzymol.* **330**, 445–454.
36. Harris, M. N., Madura, J. D., Jing, L.-J. & Harwood, V. J. (2001). Kinetic and mechanistic studies of prolyl oligopeptidase from the hyperthermophile *Pyrococcus furiosus*. *J. Biol. Chem.* **276**, 19310–19317.
37. Szeltner, Z., Renner, V. & Polgár, L. (2000). The non-catalytic β-propeller domain of prolyl oligopeptidase enhances the catalytic capability of the peptidase domain. *J. Biol. Chem.* **275**, 15000–15005.
38. Szeltner, Z., Rea, D., Juhász, T., Renner, V., Mucsi, Z., Orosz, G., Fülöp, V. & Polgár, L. (2002). Substrate-dependent competency of the catalytic triad of prolyl oligopeptidase. *J. Biol. Chem.* **277**, 44597–44605.
39. Richardson, J. S. (1981). The anatomy and taxonomy of protein structure. *Advan. Protein Chem.* **34**, 167–339.
40. Fiser, A., Cserző, M., Tüdős, É. & Simon, I. (1992). Different sequence environments of cysteines and half cystines in proteins. Application to predict disulfide forming residues. *FEBS Letters*, **302**, 117–120.
41. Kim, J.-S., Groll, M., Musiol, H.-J., Behrendt, R., Kaiser, M., Moroder, L. *et al.* (2002). Navigation inside a protease: substrate selection and product exit in the tricorn protease from *Thermoplasma acidophilum*. *J. Mol. Biol.* **324**, 1041–1050.
42. Brandstetter, H., Kim, J.-S., Groll, M., Göttig, P. & Huber, R. (2002). Structural basis for the processive protein degradation by tricorn protease. *Biol. Chem.* **383**, 1157–1165.
43. Goettig, P., Groll, M., Kim, J.-S., Huber, R. & Brandstetter, H. (2002). Structures of the tricorn-interacting aminopeptidase F1 with different ligands explain its catalytic mechanism. *EMBO J.* **21**, 5343–5352.
44. Szeltner, Z., Renner, V. & Polgár, L. (2000). Substrate- and pH-dependent contribution of oxyanion binding site to the catalysis of prolyl oligopeptidase, a paradigm of the serine oligopeptidase family. *Protein Sci.* **9**, 353–360.
45. Leatherbarrow, R. J. (2001). *GraFit, Version 5*, Erythacus Software Ltd, UK.
46. Otwinowski, Z. & Minor, W. (1997). Processing of X-ray diffraction data collected in oscillation mode. *Methods Enzymol.* **276**, 307–326.
47. Murshudov, G. N., Vagin, A. A. & Dodson, E. J. (1997). Refinement of macromolecular structures by the maximum-likelihood method. *Acta Crystallog. sect. D*, **53**, 240–255.
48. Jones, T. A., Zou, J. Y., Cowan, S. W. & Kjeldgaard, M. (1991). Improved methods for building protein models in electron density maps and the location of errors in these moldels. *Acta Crystallog. sect. A*, **47**, 110–119.
49. Szeltner, Z., Rea, D., Renner, V., Fülöp, V. & Polgár, L. (2002). Electrostatic effects and binding determinants in the catalysis of prolyl oligopeptidase. Site specific mutagenesis at the oxyanion binding site. *J. Biol. Chem.* **277**, 42613–42622.
50. Perrakis, A., Sixma, T. K., Wilson, K. S. & Lamzin, V. S. (1997). *wARP*: improvement and extension of crystallographic phases by weighted averaging of multiple-refined dummy atomic models. *Acta Crystallog. sect. D*, **53**, 448–455.
51. Read, R. J. (1986). Improved Fourier coefficients for maps using phases from partial structures with errors. *Acta Crystallog. sect. A*, **42**, 140–149.
52. Kraulis, P. J. (1991). MOLSCRIPT: a program to produce both detailed and schematic plots of protein structures. *J. Appl. Crystallog.* **24**, 946–950.
53. Esnouf, R. M. (1997). An extensively modified version of MolScript that includes greatly enhanced coloring capabilities. *J. Mol. Graph.* **15**, 133–138.
54. Brünger, A. T. (1992). Free *R* value: a novel statistical quantity for assessing the accuracy of crystal structures. *Nature*, **355**, 472–475.

Edited by R. Huber

(Received 28 January 2004; received in revised form 26 April 2004; accepted 7 May 2004)